

**IMPACT OF SILVER NANOPARTICLE EXPOSURE ON CRAYFISH
(*Orconectes virilis*) GROWTH, CHEMISTRY AND PHYSIOLOGY IN
CONTROLLED LABORATORY EXPERIMENT AND
HUDSON RIVER ECOSYSTEM**

A Final Report of the Tibor T. Polgar Fellowship Program

Allen Clayton

Polgar Fellow

School of Science, Department of Biology
Marist College
Poughkeepsie, NY 12601

Project Advisor:

Dr. Zofia Gagnon
School of Science, Department of Environmental Science
Marist College
Poughkeepsie, NY 12601

Clayton, A.C. and Z.E. Gagnon. 2012. Impact of Silver Nanoparticle Exposure on Crayfish (*Orconectes virilis*) Growth, Chemistry and Physiology in Controlled Laboratory Experiment and Hudson River Ecosystem. Section VI: 1-36 pp. In S.H. Fernald, D.J. Yozzo and H. Andreyko (eds.), Final Reports of the Tibor T. Polgar Fellowship Program, 2010. Hudson River Foundation.

ABSTRACT

The use of nanotechnology has become widespread in commercial, industrial and medical applications; however, there is concern that their high level of reactivity may also pose risks to human health and the environment. Previous studies involving metal nanoparticles have shown them to be toxic and destructive to DNA and metabolic pathways. Silver nanoparticles (AgNPs) have recently received much attention for their growing role in biotechnology and life sciences.

Crayfish (*Orconectes virilis*), a common inhabitant of the Hudson River and its tributaries, were used as an experimental model in this project. A colloidal solution of AgNPs was synthesized from chemical reduction of silver nitrate (AgNO_3) by sodium borohydride (NaBH_4), and organisms were exposed for 10 days to different concentrations of colloidal AgNP suspended in Hudson River water. The following AgNP concentrations were used: 0.0, 0.05, 0.107, 0.16, and 0.214 mg/L. Control treatments of AgNO_3 and NaBH_4 were established in the same concentrations used for synthesis of the AgNP treatments. Additional control treatments were established using untreated Hudson River water, and cages placed directly in the Hudson River (river control). Crayfish were harvested and examined for silver accumulation, DNA damage, and pathological changes. Silver accumulation in major organs was determined by atomic absorption using a ThermoElemental Solaar M5 spectrophotometer in graphite furnace mode. DNA damage was examined via single cell gel electrophoresis (comet assay).

The bioaccumulation of Ag in crayfish liver, muscle, and green gland tissues was detected in all AgNP and AgNO_3 treatments. DNA damage was found to be statistically significant in all laboratory specimens when compared to the river control.

TABLE OF CONTENTS

Abstract.....	VI – 2
Table of Contents.....	VI – 3
List of Tables and Figures.....	VI – 4
Introduction.....	VI – 6
Methods.....	VI – 10
Results.....	VI – 18
Discussion.....	VI – 29
Conclusions and Recommendations.....	VI – 31
Acknowledgments.....	VI – 33
Literature Cited.....	VI – 34

LIST OF TABLES AND FIGURES

Table 1 - The schematic of compound amounts used in the synthesis of colloidal AgNPs and AgNP concentrations obtained in the process of synthesis	VI-12
Table 2 - Treatments and Experimental Design	VI-14
Figure 1 - Mortality of crayfish in different experimental treatments. The bar graphs represent total number of organisms that died during treatment exposure. The values were obtained by pooling all the organisms that died at specific Concentrations	VI-18
Table 3 - Average weight loss of crayfish in different experimental exposures. The values in the table represent average measurements of all 6 organisms per treatment recorded at the beginning of the experiment (June 20) and compared to the weight at the end of the experiment (June 30)	VI-19
Figure 2 - AgNP induced DNA damage in crayfish brain tissues expressed as length of DNA comet tail. The bar graphs represent comet length means \pm SD of ~50 nuclei per sample from each specimen.....	VI-20
Figure 3 - AgNO ₃ induced DNA damage in crayfish brain tissues expressed as length of DNA comet tail. The bar graphs represent comet length means \pm SD of ~50 nuclei per sample from each specimen.....	VI-21
Figure 4 - NaBH ₄ induced DNA damage in crayfish brain tissues expressed as length of DNA comet tail. The bar graphs represent comet length means \pm SD of ~50 nuclei per sample from each specimen.....	VI-21
Figure 5a - Total amount of Ag (μ g/g dry w.) accumulated in crayfish liver tissue in NaBH ₄ treatments as determined by GFAAS measurements. The bar graphs represent Ag content means \pm SD of three measurements.....	VI-23
Figure 5b - Total amount of Ag (μ g/g dry w.) accumulated in crayfish liver tissue in AgNO ₃ treatments as determined by GFAAS measurements. The bar graphs represent Ag content means \pm SD of three measurements.....	VI-23
Figure 5c - Total amount of Ag (μ g/g dry w.) accumulated in crayfish liver tissue in AgNP treatments as determined by GFAAS measurements. The bar graphs represent Ag content means \pm SD of three measurements.....	VI-24
Figure 6a - Total amount of Ag (μ g/g dry w.) accumulated in crayfish green gland tissue in NaBH ₄ treatments as determined by GFAAS measurements. The bar graphs represent Ag content mean \pm SD of three measurements.....	VI-25

Figure 6b – Total amount of Ag ($\mu\text{g/g}$ dry w.) accumulated in crayfish green gland tissue in AgNO_3 treatments as determined by GFAAS measurements. The bar graphs represent Ag content mean \pm SD of three measurementsVI-26

Figure 6c - Total amount of Ag ($\mu\text{g/g}$ dry w.) accumulated in crayfish green gland tissue in AgNP treatments as determined by GFAAS measurements. The bar graphs represent Ag content mean \pm SD of three measurementsVI-26

Figure 7a - Total amount of Ag ($\mu\text{g/g}$ dry w.) accumulated in crayfish muscle tissue in NaBH_4 treatments as determined by GFAAS measurements. The bar graphs represent Ag content mean \pm SD of three measurementsVI-27

Figure 7b - Total amount of Ag ($\mu\text{g/g}$ dry w.) accumulated in crayfish muscle tissue in AgNO_3 treatments as determined by GFAAS measurements. The bar graphs represent Ag content mean \pm SD of three measurementsVI-28

Figure 7c - Total amount of Ag ($\mu\text{g/g}$ dry w.) accumulated in crayfish muscle tissue in AgNP treatments as determined by GFAAS measurements. The bar graphs represent Ag content mean \pm SD of three measurementsVI-29

Figure 8 - Hypothetical dose response to illustrate a nonconventional dose responseVI-30

INTRODUCTION

The use of nanotechnology has grown dramatically in commercial, industrial, medical, and consumer products in the last decade. The National Science and Technology Council in 2001 defined the scale of nanotechnology as atomic, molecular or macromolecular levels in the range of $\sim 1 - 100$ nanometers (Hornyak et al. 2009). The National Nanotechnology Initiative, established in 2001, led to public funding for nanoparticle (NP) research in the United States to develop new material applications and to investigate new commercial applications for NP antimicrobial capability (Ahamed et al. 2008). Metal oxide NPs currently have wide industrial applications in photocatalytic water purification systems (Hagfeldt and Graetzel 1995), solar cells (Usui et al. 2004), electronics, and many everyday products such as sunscreens and cosmetics. NPs also have exceptionally desirable biological, fungicidal, bacteriological, and algicidal properties. Today, development of a NP application is frequently considered an advancement of modern science.

Silver nanoparticles (AgNPs) have recently received broad attention for their growing role in biotechnology and life science. Among 580 consumer nanotechnology-based products, the most common material mentioned in product descriptions is silver-based nanoparticles (Woodrow Wilson Center 2007; Henig 2007). AgNPs have a large surface area relative to their volume and, as a result of their size, easily interact with other particles (Ying 2001). AgNPs are used to technologically enhance products such as bandages, clothing, cosmetics, food, and toys (Woodrow Wilson Center 2007; Henig 2007). The antibacterial effect of AgNPs has brought about their extensive use in health, electronic, and home goods. Recently, AgNPs have been used in the production of

clothing and food products to reduce bacterial growth (Chau et al. 2007; Vigneshwaran et al. 2007). AgNPs are used as an antimicrobial agent in consumer goods such as disinfectants, deodorants, toothpaste, shampoo, and humidifiers (Woodrow Wilson Center 2007; Henig 2007). AgNPs are proven to be very effective bacterial filters. It has been suggested that AgNPs be added to aquaculture systems for use as anti-bacterial and anti-fungal agents in wastewater treatment plants. However, researchers have found that nanoparticles also eliminate helpful bacteria that remove ammonia, and lethal toxicity levels of NPs are still under debate (Choi and Hu 2008).

AgNPs are also of interest to defense and engineering programs for new material applications (Ringer and Ratinac 2004). There is a potential for AgNPs to be an ingredient in the treatment of diseases that need constant drug concentration in the blood or to target specific cells or organs (Moghimi et al. 2001; Panyam and Labhasetwar 2003). *In vitro* tests have shown that AgNPs can be used to inhibit binding of the HIV-1 virus to host cells (Ahamed et al. 2008; Elechiguerra et al. 2005). Medicinally, antimicrobial activity of AgNPs has been used to reduce infections in burn treatment (Kim et al. 2007; Ulkur et al. 2005) and to reduce the risk of infection by treating the surface of catheters (Samuel and Guggenbichler 2004), prostheses (Gosheger et al. 2004), and human skin (Paddle-Ledinek et al. 2006).

Regardless of the prevalent application of AgNPs, there is a lack of information relating to their toxicity at the organismal, cellular, and molecular level (Ahamed et al. 2008). The concentrations at which AgNPs become toxic are currently being determined. Mnyusiwalla et al. (2003) expressed concern that NPs could have potentially adverse effects on human health and the environment. The high surface to volume ratio gives NPs

catalytic qualities, and their size allows them to pass through cell membranes with currently unknown biological effects (The Center for Food Safety 2006).

Sung et al. (2008) conducted an extensive study on inhalation exposure of AgNPs using Sprague-Dawley strain rats. Histopathological examinations indicated that inflammatory cell infiltrate, chronic alveolar inflammation, and small granulomatous lesions were proportionally correlated to AgNP dose. The exposure influenced minimal bile-duct hyperplasia in males and females, chronic alveolar inflammation and macrophage accumulation in the lungs of males and females, and erythrocyte aggregation in females. However, the authors of the study reported that an exposure level of 100 $\mu\text{g}/\text{m}^3$ had no adverse effect on experimental animals, which was consistent with the American Council of Government Industrial Hygienists silver dust threshold limit value (TLV).

In studies on mammal germ line stem cells, AgNPs have been shown to decrease mitochondrial activity and increase membrane leakage. In addition, AgNPs were found to increase the creation of reactive oxygen species (ROS), reduce antioxidant activity of glutathione (GSH), and diminish mitochondrial function in Buffalo rat liver (BRL-3A) cells (Ahamed et al. 2008; Braydich-Stolle et al. 2005; Hussain et al. 2005). Studies were done to observe DNA damage in response to polysaccharide surface functionalized (coated) and non-functionalized (uncoated) AgNPs in two types of mammalian cells, including mouse embryonic stem (mES) cells and mouse embryonic fibroblasts (MEF) (Ahamed et al. 2008). The experiment showed more severe damage in coated AgNPs, suggesting that genotoxicity may be affected by different AgNP surface chemistry (Ahamed et al. 2008).

Another experiment on AgNPs studied the lipid-based dispersion of NPs, sometimes helpful in reducing nanoparticle toxicity and in developing therapeutic agents (Bothun 2008). Accommodation of large hydrophobic NPs in lipid bilayers was confirmed. It appears that this is done by distortion of lipid bilayers relative to the thickness of the bilayer (Bothun 2008).

Blood hematology and biochemistry were analyzed and the results found significant dose-dependent changes on alkaline phosphates and cholesterol values for both male and female rats, implying slight liver damage from AgNP inhalation exposures of more than 300 mg (Kim et al. 2007). The study showed accumulation of AgNPs was more significant in female kidneys than in male kidneys. Conclusions were made that prolonged AgNP inhalation exposure would significantly increase the occurrence of lung inflammation, at much lower mass dose concentrations, when compared to submicrometer particles (Sung et al. 2008).

The safety of NP topical use has also become of great interest. There is very little known about their potential to penetrate the skin. Larese et al. (2009) evaluated *in vitro* skin penetration of AgNPs coated with polyvinylpyrrolidone (PVP). The experiments were done using the Franz diffusion cell method with intact and damaged human skin. AgNP absorption through intact and damaged skin was detectable by electron microscopy in the stratum corneum and the outermost surface of the epidermis (Larese et al. 2009).

The very limited knowledge on toxicological risk assessment of engineered NPs to biological systems raises public and scientific concern. Questions regarding NPs associated with commonly used nanotechnology, particularly how much eventually enters

the environment, remain unanswered. Of even greater concern, and poorly understood, is the potential effect on human health and the fate of nanomaterials in terrestrial and aquatic environments (Hornyak et al. 2009). Since there are no existing methods for removal of AgNPs from wastewater effluents (Hornyak et al. 2009), it is especially urgent to learn how much silver (Ag) from colloidal AgNP suspensions is being introduced into waterways.

The purpose of this project was to study the effect of AgNP exposure on an aquatic animal, using crayfish (*Orconectes virilis*) as experimental model. Crayfish is a common inhabitant of the Hudson River Watershed and known not to tolerate polluted water. In this study, crayfish were exposed to varying levels of colloidal AgNPs in Hudson River water culture media to test the hypothesis that exposure would be correlated with bioaccumulation of Ag in animal tissues, pathological changes, and DNA damage. An additional control group of caged crayfish was placed directly in the Hudson River (river control) during the experimental period to compare laboratory findings with a natural environment.

METHODS

Experimental Organism

The crayfish (*Orconectes virilis*), a common inhabitant of the Hudson River and its tributaries, was chosen as the experimental organism because it lives in the sediment where most pollutants accumulate. The stock used in the experiment consisted of crayfish specimens purchased from Northeastern Aquatics in Rhinebeck, NY.

Hudson River Water Dechlorination and Filtration

The aquaria were filled with 20 L of raw, unfiltered Hudson River water. Upon trial tests of the addition of AgNO_3 , NaBH_4 , and AgNP , the AgNO_3 water became light pink which progressed to red and eventually black. The CRC Handbook of Chemistry and Physics was consulted, and it was determined that the coloration was due to the formation of the chemical, AgCl . A colormetric test was conducted on untreated Hudson River water, and free Cl was found to be 0.070mg/L . It turns out that the Marist College River Lab is located approximately 300 yards down river from the Poughkeepsie Water Treatment Plant, the apparent source of the chlorine. Due to AgNO_3 's high reactivity, all water used in the experiment was allowed to dechlorinate for one week. A separate aquarium was completely filled with raw Hudson River water to serve as a fresh supply of dechlorinated water to keep each tank's water level at 20 L. The contents of the tanks were filtered during the dechlorination period with a Lee's Economy Corner Filter filled with filter floss for particulates only. Filter floss was replaced on the second, fourth, and seventh days. Due to its highly absorptive nature and ability to remove metals, activated charcoal filters were avoided in the experiment (Bansal and Goyal 2005). The filters were powered using Tetra Whisper aquarium tank air pumps.

Aquaria Preparation

After the dechlorination period, three cups of quarter inch aquarium stone were placed on the bottom as substrate. Three five-inch pieces of 2 in. diameter PVC cut in half lengthwise were placed on the substrate as a shelter for the crayfish.

Crayfish Acclimation

Upon arrival, three experimental organisms were placed in each tank and allowed to acclimate to the laboratory and Hudson River conditions for one week. From the 120 crayfish purchased, 96 specimens were chosen at random, while at the same time trying to obtain organisms of relatively the same age and size. Crayfish were fed dry cat food (one piece per organism). Any excess food was immediately removed from the aquarium. No ammonia filtration was required due to the low amount of liquid waste produced by the crayfish and the short, ten day exposure time.

Nanoparticle Synthesis

During the acclimation period, the AgNPs were synthesized. A slightly modified Creighton method of AgNP synthesis was used for the experiment (Creighton and Eadon 1991). AgNPs were synthesized through the chemical reduction of silver nitrate (AgNO_3) using sodium borohydride (NaBH_4) as a reducing agent. AgNPs are an aggregation of elemental Ag that forms together in a spherical structure, each structure from 1 to 100 nm. An AgNO_3 solution (3.4 mg in 20 ml deionized water) cooled to approximately 10°C

Table 1. The schematic of compound amounts used in the synthesis of colloidal AgNPs and AgNP concentrations obtained in the process of synthesis.

Synthesis Formula			Concentration
AgNO_3 (mg)	NaBH_4 (mg)	AgNP (ml)	Ag mg/L
3.4	4.5	80	0.107
Breakdown of Concentrations (mg/L)			Final Concentrations
1.7	2.3	40	0.05
3.4	4.5	80	0.107
5.1	6.8	120	0.16
6.8	9.0	160	0.214

was added drop wise with constant stirring to a NaBH₄ solution (4.53 mg in 60 ml deionized water) pre-cooled to 2°C. Table 1 summarizes compound amounts used to synthesize the resulting Ag concentrations used for treatments. Stirring continued for about 45 minutes. A 250 ml Erlenmeyer flask in which the reaction was taking place was wrapped in aluminum foil to block light (the reaction is light sensitive).

Following the synthesis process, the solution remained on ice and stirred for 1h. The ice bath was removed and the AgNPs remained on the stir plate until they reached room temperature. All treatment solutions were then stored at 5°C.

Experimental Setup

After the acclimation period, each tank was refilled with dechlorinated Hudson River water up to the 20 L mark and the weight of each organism was recorded to the nearest tenth of a gram. Specimens in each tank were marked with a red dot, a yellow dot, or no color to distinguish between the three specimens. As noted in Table 1, Ag concentrations of 0.05, 0.107, 0.16, and 0.214 mg/L were established by adding the following amounts of stock AgNP solution, 40.0 ml, 80.0 ml, 120.0 ml and 160.0 ml, to 20 L of Hudson River water. The corresponding control treatments of AgNO₃ and NaBH₄ (parental compound) in the same concentrations as AgNP were also established, as shown in Table 2. Each treatment was applied to two separate tanks resulting in six total crayfish replicates per treatment. There were eight tanks per generic treatment resulting in 24 treated tanks. Along with the two control tanks containing only filtered and dechlorinated Hudson River water (laboratory control), there were also two sets of three specimens in cages suspended in the Hudson River which served as a natural, non-laboratory control (river control). In addition to the laboratory and river controls,

controls were established for the paternal materials, AgNO₃ and NaBH₄, from which AgNPs were synthesized. This was done because there is some evidence that AgNPs in colloidal solution can deaggregate to form their original compounds. Deaggregates can be identified in the solutions as described by Jayabalan et al. (2008). The concentrations of these controls were calculated based on the amount used for the synthesis of AgNPs.

Table 2. Treatments and Experimental Design

Treatment No.	Treatment Concentration	Number of Specimens
Laboratory Experiment		
1	0.050 mg/L AgNP ¹	6
2	0.107 mg/L AgNP	6
3	0.160 mg/L AgNP	6
4	0.214 mg/L AgNP	6
5	Laboratory Control (Hudson River water)	6
AgNO ₃ Controls		
6	0.085 mg/L AgNO ₃ ²	6
7	0.170 mg/L AgNO ₃	6
8	0.270 mg/L AgNO ₃	6
9	0.340 mg/L AgNO ₃	6
NaBH ₄ Controls		
10	0.115 mg/L NaBH ₄ ³	6
11	0.225 mg/L NaBH ₄	6
12	0.340 mg/L NaBH ₄	6
13	0.450 mg/L NaBH ₄	6
Hudson River Control		
14	Cages suspended directly in Hudson River	6

¹100 ppm concentration of AgNP was determined in the experiments as LD₅₀ (lethal dose to 50% of chick embryos in earlier preliminary experiments conducted at Marist College)

² AgNO₃ control concentrations were based on concentration of Ag ion, see: Synthesis of Silver Nanoparticles (AgNPs) and Controls.

³NaBH₄ control concentrations based on B (boron) ion, see: Synthesis of Silver Nanoparticles (AgNPs) and Controls.

Gross and Behavioral Observations

The lab specimens were checked for responsiveness to a threat and to food. A piece of sinking wafer food was broken in half and dropped in front of each crayfish. Responsiveness was gauged not by whether or not the food was immediately eaten, but rather by the movement of the mouth. If the mouth appendages began to flutter when food was placed in the tank, they were said to be responsive to food. Fear response was gauged by poking a 12 inch glass stirring rod at the crayfish. If the specimen flipped its tail quickly in a manner similar to escape, they were said to be responsive to fear. Each day the tanks were refilled to the 20 L mark and the specimens were fed and checked for any change in behavior or for death. Any dead organism found within the acclimation period was replaced. Organisms that died after the treatments were administered were removed from the tank and not processed in the results. The replacement crayfish were weighed before being placed into the tank. On the final day of the exposure period all crayfish were again weighed using the same method as with the initial weights.

Tissue Sampling

The experiment was terminated on the 10th day of exposure. On the morning of harvest, all crayfish were put into bags labeled according to their tank and treatment and placed on ice for 1 minute to anesthetize them. A specimen was removed from a bag and surgically decapitated within 5-10 seconds to avoid major stress. The organs harvested included: brain, gills, liver, green gland, nerve ganglia, heart, and tail muscle. Samples of brain and liver chosen at random were immediately processed and analyzed for DNA damage. Samples of liver, green glands, and tail muscles were placed in a drying oven at 80°C for chemical analysis of Ag content.

DNA Analysis by Single Gel Electrophoresis (Comet Assay)

At the time of dissection, one brain and one liver sample per tank (two per treatment) were immediately processed for DNA damage. The tissue was minced in a 20 mM solution of EDTA in PBS to release cell nuclei. Minced tissue was placed in fresh solution of 20 mM EDTA and centrifuged for eight minutes. Ten microliters of supernatant was drawn off immediately above the pellet. This was mixed with 90 μ l of low melting agar. The 100 μ l solution was placed on a pre-treated comet assay slide (Trevigen[®]). The slide was placed in an alkaline solution of pH 13 to unwind the DNA for 30 minutes. Slides were then placed in CometAssay[™] Electrophoresis System (Trevigen[®]) in electrophoresis buffer (pH >13) and was carried out for 30 minutes. After this time, the slides were placed in 70% alcohol for five minutes and allowed to air dry overnight. Extracted DNA on the slides was stained with SYBR-green[™], which emits fluorescent light within the 425-500 nm region. The slides were analyzed under a mercury lit epifluorescent microscope. A Magnafire SP Digital Camera was used to take pictures of comets viewed with the microscope. Length of DNA (comet) migration was measured using Image-Pro[®] Plus software. All nuclei and their comets on the slides were measured (~50). Distribution of DNA between the tail and head of the comet was used to evaluate the degree of DNA damage. Measurements were recorded on nuclei with clearly defined tail boundaries.

Atomic Absorption Analysis

Samples of muscle, liver, and green gland tissue were oven dried for 72 hours at 80°C. The tissue was ground to a fine powder using mortar and pestle, and samples were weighted to obtain ~0.1g.

In preparation for chemical digestion, tissues were placed in an Xpress vessel with 5 ml of high purity nitric acid (Fisher Scientific, Optima Grade). Chemical digestion was performed using the MARS Xpress microwave (CEM). The process parameters were set to 180 °C operating temperature, 80 watts, ten minute ramp to temperature, and ten minute run time. The digestion program was run for 30 minutes.

Silver content analyses were conducted via atomic absorption (AA) spectrometry using a ThermoElemental Solaar M5 atomic spectrophotometer in graphite furnace mode (GFAAS). Reference 1.0 ppm Ag standard was prepared using a 1.0×10^3 ppm Ag solution purchased from Fisher Scientific (Lot # CL4-132AG) and certified by SPEX CertiPrep. The absorption wavelength of Ag was 328.1 nm, and the temperature was 2500°C. Ag concentrations were established through external calibration standards using a least squares fit regression curve. Results given by the AA computer output were in units of µg/L. Calculations were made to determine the Ag content in the 1 g dry weight of the sample [g (AgNP)/g tissue].

Trace levels of Ag in NaBH₄ treatment samples was observed. It was determined that the NPs persisted in the nalgene cuvettes after the digestion process. Ag contamination was essentially eliminated by rinsing cuvettes twice with 5 ml of 50% HNO₃, then microwaving the empty cuvettes. Cuvettes were then rinsed twice with deionized water.

Statistical Analysis

The SPSS (ver. 16.0, 2007) statistical package was used to analyze data collected on comet tail length (DNA damage) and Ag content in the tissue. Analyses of AgNP accumulation for the different treatment concentrations in the liver, green gland, and muscle tissue were also performed. Analysis of variance (ANOVA) followed by the

Student-Newman-Keuls multiple comparison procedure was used to conclude the variation in comet tail length and accumulation of Ag levels at probability level $\alpha \leq 0.05$.

RESULTS

Crayfish Mortality

Figure 1 represents the mortality of crayfish exposed to different treatments. The highest mortality was observed in AgNO_3 treatments. A total of 10 crayfish died in AgNO_3 treatments, three crayfish died in AgNP treatment exposures, one died in the NaBH_4 treatments, and one in the laboratory control treatment. No deaths occurred in the river control.

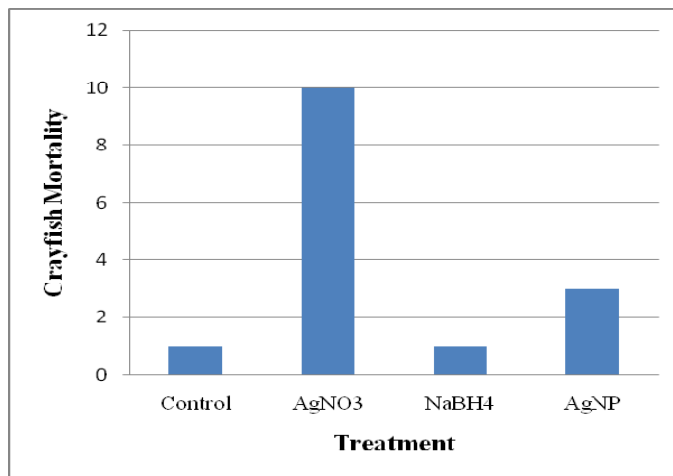


Figure 1. Mortality of crayfish in different experimental treatments. The bar graphs represent total number of organisms that died during treatment exposure. The values were obtained by pooling all the organisms that died at specific concentrations. All deaths were recorded after treatments were administered.

Table 3. Average weight loss of crayfish in different experimental exposures. The values in the table represent average measurements of all 6 organisms per treatment recorded at the beginning of the experiment (June 20) and compared to the weight at the end of the experiment (June 30).

Treatment	Initial Avg Weights (g)	Final Avg Weights (g)	Weight Change (g)
Lab Control	26.2	25.4	-0.8
AgNO ₃	20.3	19.3	-1.0
NaBH ₄	17.1	16.7	-0.4
AgNP	16.2	14.2	-2.0

Gross Pathology

Our observations revealed that crayfish in AgNP demonstrated the largest change in weight (Table 3).

Behavioral Changes

Recorded visual observations and external stimuli showed the crayfish in the AgNO₃ became very lethargic and unresponsive to both food and threat. Organisms in the NaBH₄ sporadically would not respond to food, but always to threat. Organisms treated with AgNP remained responsive to food and threat throughout the experiment.

DNA Analysis

Brain: Results of exposure to treatments, AgNP and the paternal materials AgNO₃ and NaBH₄, are represented in Figures 2, 3 and 4. All figures show the statistically significant difference in DNA damage between the river control and the laboratory (lab) control as measured by DNA migration (comet tail length). DNA damage was not observed in the river control samples.

As shown in Figure 2, the extent of DNA migration in the AgNP treatments increased significantly in all concentrations in comparison to the controls ($\alpha \leq 0.05$). There was no statistically significant difference in comet tail length between the 0.05,

0.107, and 0.214 AgNP treatment concentrations; however, comet tail length in the 0.16 mg/L AgNP treatment concentration increased significantly when compared to the other three AgNP treatment concentrations ($\alpha \leq 0.05$). Comet length in the 0.16 mg/L AgNP treatment concentration increased 46% in comparison to the lab control.

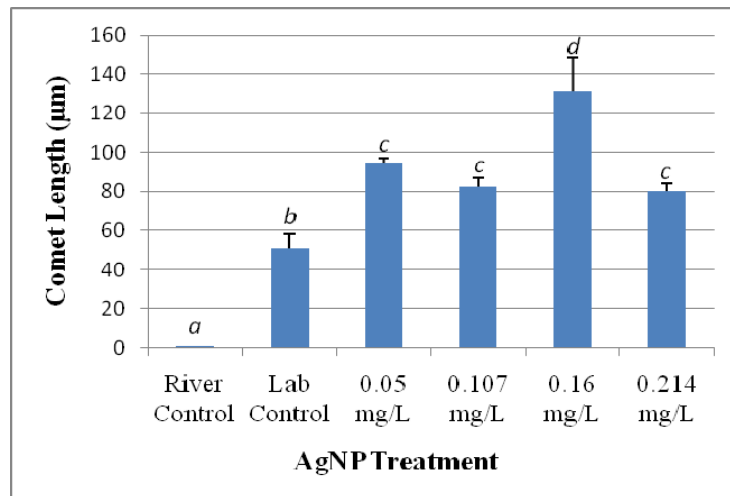


Figure 2. AgNP induced DNA damage in crayfish brain tissues expressed as length of DNA comet tail. The bar graphs represent comet length means \pm SD of \sim 50 nuclei per sample from each specimen. Columns with different letters (*a, b, c, d*) are significantly different at probability level $\alpha \leq 0.05$ as determined by multiple comparison test Student-Newman-Keuls (SPSS 16.0).

Figure 3 shows that when comparing the AgNO₃ treatments to the lab control, there was a statistically significant difference between the comet tail lengths measured in the 0.085, 0.17, and 0.34 mg/L treatments ($\alpha \leq 0.05$). However, comet tail lengths in the 0.27 mg/L AgNO₃ treatment were not significantly different to those measured in lab control or to the other three AgNO₃ treatments.

As shown in Figure 4, there was a statistically significant increase in comet tail length when comparing the lab control to the 0.115 and 0.225 mg/L NaBH₄ treatments; however, there was no significant difference between those two NaBH₄ treatments. DNA

damage in the 0.34 and 0.45 concentrations was too extensive and the resulting comet tail was too diffuse for an image to be measured by the Image-Pro® Plus software.

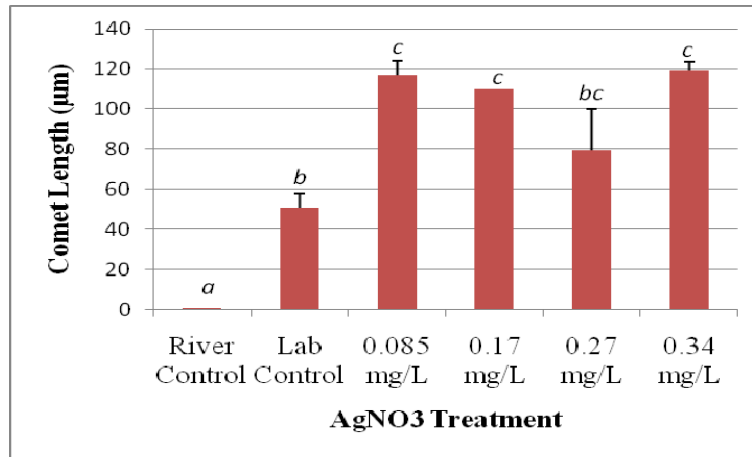


Figure 3. AgNO₃ induced DNA damage in crayfish brain tissues expressed as length of DNA comet tail. The bar graphs represent comet length means ±SD of ~50 nuclei per sample from each specimen. Columns with different letters (*a, b, c, d*) are significantly different at probability level $\alpha \leq 0.05$ as determined by multiple comparison test Student-Newman-Keuls (SPSS 16.0).

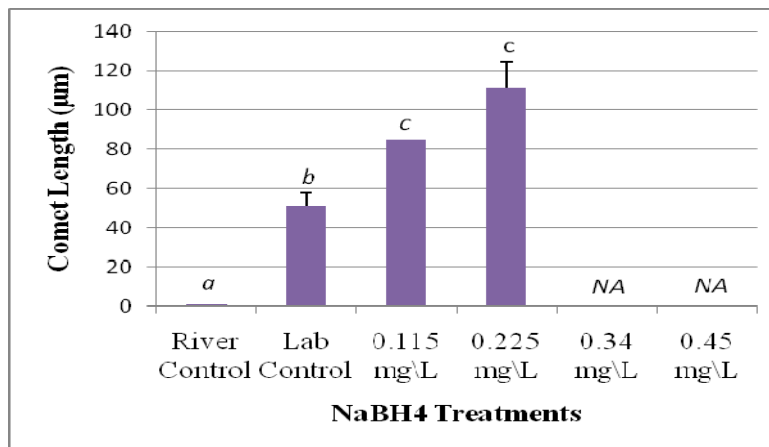


Figure 4. NaBH₄ induced DNA damage in crayfish brain tissues expressed as length of DNA comet tail. The bar graphs represent comet length means ±SD are average length of ~50 nuclei per sample from each specimen. Columns with different letters (*a, b, c*) are significantly different at probability level $\alpha \leq 0.05$ as determined by multiple comparison test Student-Newman-Keuls (SPSS 16.0). Measurements in the NA concentrations were immeasurable with available equipment because of extreme dispersal of DNA.

Atomic Absorption Analysis

The results of atomic absorption analysis of Ag content in liver, green gland, and muscle tissues are shown in Figures 5a, 5b, 5c, 6a, 6b, 6c, 7a, 7b, and 7c. Each sample was measured three times, and the absorbance values were averaged before extrapolating the Ag concentration from the calibration curve. Calibrations were performed using acid-matched standard solutions of Silver Standard. Metal concentrations were determined through external calibration, with standards using least-squares fit of regression curves. Chemical analysis of the liver, green gland, and muscle tissues in river control specimens did not detect any presence of Ag.

Liver: Figures 5a-5c represent the Ag content determined in crayfish liver samples. The figures show that there was no statistically significant difference in Ag content detected in lab control tissue samples when compared to river control samples.

Figure 5a illustrates results from the NaBH₄ treatments. There was a trace amount of Ag detected in liver tissue in the highest concentration, 0.214 mg/L, although no Ag was in the treatment. The amount of Ag in NaBH₄ could be the result of contamination during tissue processing.

Figure 5b presents Ag content in liver tissue in the AgNO₃ treatments. There was statistically significant accumulation of Ag in the liver tissue in the lowest (0.085 mg/L) and the highest (0.34 mg/L) AgNO₃ treatments when compared to the controls and remaining treatments ($\alpha \leq 0.05$). There was no significant difference in Ag accumulation between the river control, lab control, 0.17 mg/L, and 0.27 mg/L treatments. In addition, there was a statistically significant difference in Ag accumulation in the 0.34 mg/L concentration treatment when compared to the 0.085 mg/L treatment concentration.

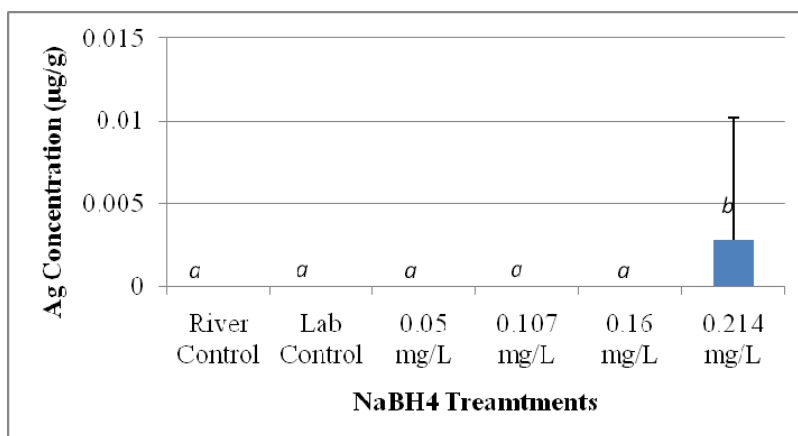


Figure 5a. Total amount of Ag ($\mu\text{g/g}$ dry w.) accumulated in crayfish liver tissue in NaBH_4 treatments as determined by GFAAS measurements. The bar graphs represent Ag content means \pm SD of three measurements. Columns with different letters (*a*, *b*) are significantly different at probability level $\alpha \leq 0.05$ as determined by multiple comparison test Student-Newman-Keuls (SPSS 16.0).

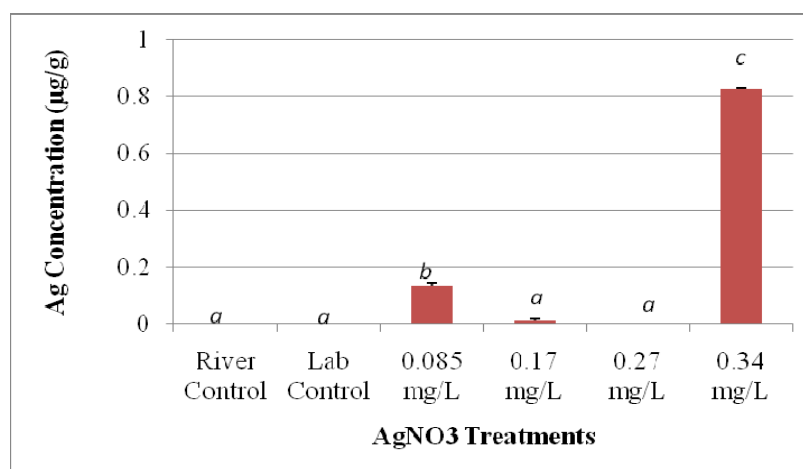


Figure 5b. Total amount of Ag ($\mu\text{g/g}$ dry w.) accumulated in crayfish liver tissue in AgNO_3 treatments as determined by GFAAS measurements. The bar graphs represent Ag content means \pm SD of three measurements. Columns with different letters (*a*, *b*, *c*) are significantly different at probability level $\alpha \leq 0.05$ as determined by multiple comparison test Student-Newman-Keuls (SPSS 16.0).

Atomic absorption analysis demonstrated increasing Ag accumulation in the crayfish liver tissues with increasing AgNP treatment concentration (Figure 5c). The

accumulation was not statistically significant for the 0.05 mg/L AgNP treatment concentration when compared to the river and lab controls ($\alpha \leq 0.05$); however, Ag accumulation was statistically significant for the 0.107, 0.16, and 0.214 mg/L concentration treatments. Additionally, each AgNP treatment demonstrated statistically significant accumulation results when compared to the other three AgNP treatments.

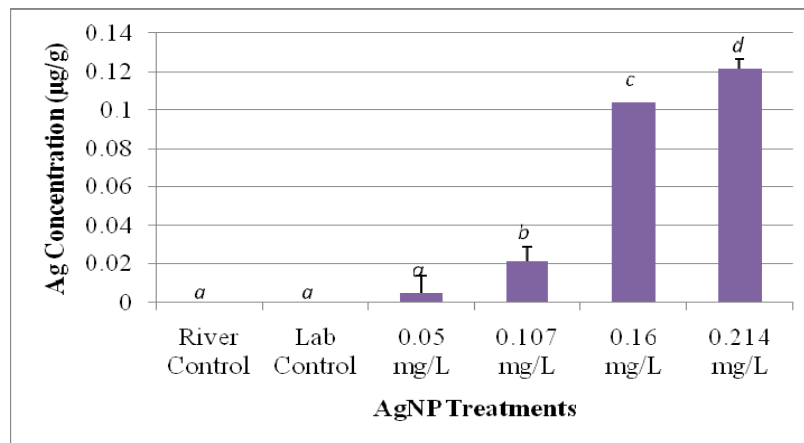


Figure 5c. Total amount of Ag ($\mu\text{g/g}$ dry w.) accumulated in crayfish liver tissue in AgNP treatments as determined by GFAAS measurements. The bar graphs represent Ag content means \pm SD of three measurements. Columns with different letters (*a*, *b*, *c*, *d*) are significantly different at probability level $\alpha \leq 0.05$ as determined by multiple comparison test Student-Newman-Keuls (SPSS 16.0).

Green Gland: Figures 6a-6c represent Ag content in the crayfish green gland tissues. The pair of kidney-like green glands play a very important excretory function. The figures show that there was a statistically significant difference in Ag content detected in lab control samples when compared to river control samples.

Figure 6a shows that there was Ag present in the green glands of crayfish in the NaBH_4 treatments. It may be that accumulation of Ag in these treatments resulted from sample contamination.

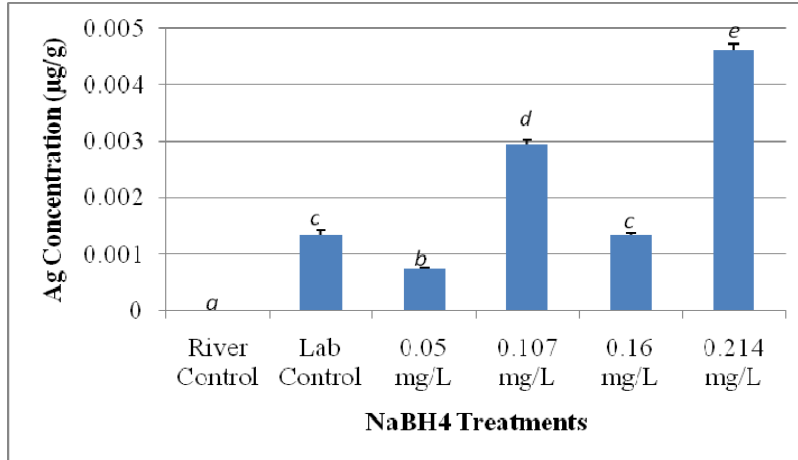


Figure 6a. Total amount of Ag ($\mu\text{g/g}$ dry w.) accumulated in crayfish green gland tissue in NaBH_4 treatments as determined by GFAAS measurements. The bar graphs represent Ag content means \pm SD of three measurements. Columns with different letters (*a, b, c, d, e*) are significantly different at probability level $\alpha \leq 0.05$ as determined by multiple comparison test Student-Newman-Keuls (SPSS 16.0). Each value is the mean of three measurements.

As can be seen in Figure 6b, the AgNO_3 treatments demonstrated statistically significant differences in Ag content in the 0.085, 0.27, and 0.34 mg/L concentration treatments when compared to the river control ($\alpha \leq 0.05$). No statistically significant difference was found between the lab control and the 0.27 mg/L concentration treatment. Additionally, each AgNO_3 treatment demonstrated statistically significant accumulation results when compared to the other three AgNO_3 treatments.

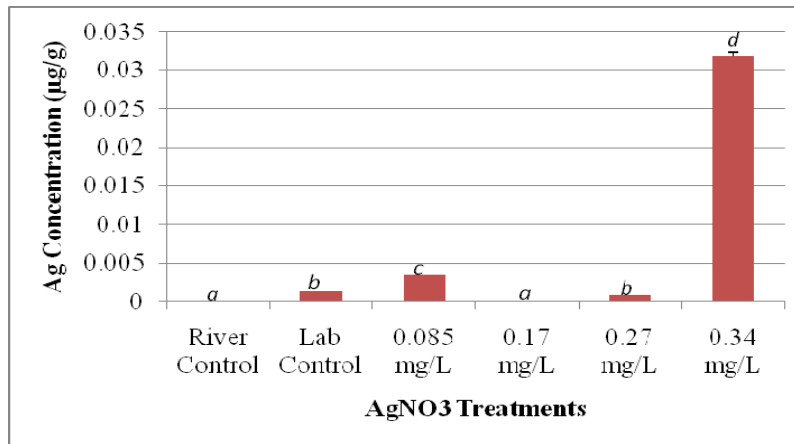


Figure 6b. Total amount of Ag ($\mu\text{g/g}$ dry w.) accumulated in crayfish green gland tissue in AgNO_3 treatments as determined by GFAAS measurements. The bar graphs represent Ag content means \pm SD of three measurements. Columns with different letters (*a*, *b*, *c*, *d*) are significantly different at probability level $\alpha \leq 0.05$ as determined by multiple comparison test Student-Newman-Keuls (SPSS 16.0). Each value is the mean of three measurements.

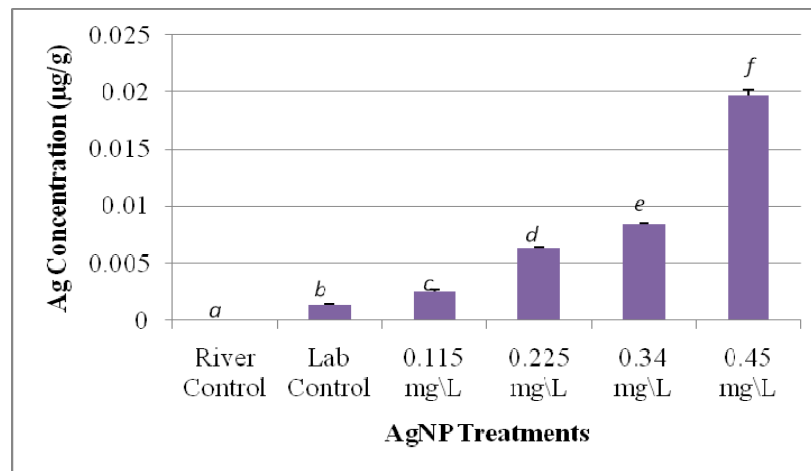


Figure 6c. Total amount of Ag ($\mu\text{g/g}$ dry w.) accumulated in crayfish green gland tissue in AgNP treatments as determined by GFAAS measurements. The bar graphs represent Ag content means \pm SD of three measurements. Columns with different letters (*a*, *b*, *c*, *d*, *e*, *f*) are significantly different at probability level $\alpha \leq 0.05$ as determined by multiple comparison test Student-Newman-Keuls (SPSS 16.0). Each value is the mean of three measurements.

Figure 6c shows statistically significant different Ag content levels in all AgNP treatments when compared to river control and lab ($\alpha \leq 0.05$). Additionally, each AgNP treatment demonstrated statistically significant accumulation results when compared to the other three AgNP treatments.

Muscle: Figures 7a-7c represent Ag accumulation in the crayfish tail muscle. The figures show that there was a statistically significant difference in Ag content detected in lab control tissue samples when compared to river control samples. A trace amount of silver was detected in the NaBH_4 treatments (Figure 7a), which may be attributed to contamination.

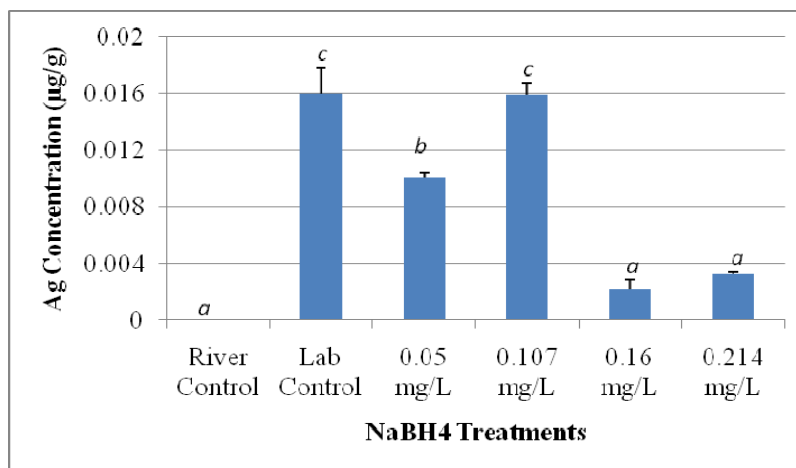


Figure 7a. Total amount of Ag ($\mu\text{g/g}$ dry w.) accumulated in crayfish muscle tissue in NaBH_4 treatments as determined by GFAAS measurements. The bar graphs represent Ag content means \pm SD of three measurements. Columns with different letters (*a*, *b*, *c*) are significantly different at probability level $\alpha \leq 0.05$ as determined by multiple comparison test Student-Newman-Keuls (SPSS 16.0). Each value is the mean of three measurements.

It can be seen in Figure 7b that all AgNO_3 treatments demonstrated statistically significant differences in Ag content when compared to the river control ($\alpha \leq 0.05$). No significant difference was found between the lab control and the 0.085 mg/L

concentration treatment. Additionally, each AgNO₃ treatment demonstrated statistically significant accumulation results when compared to the other three AgNO₃ treatments.

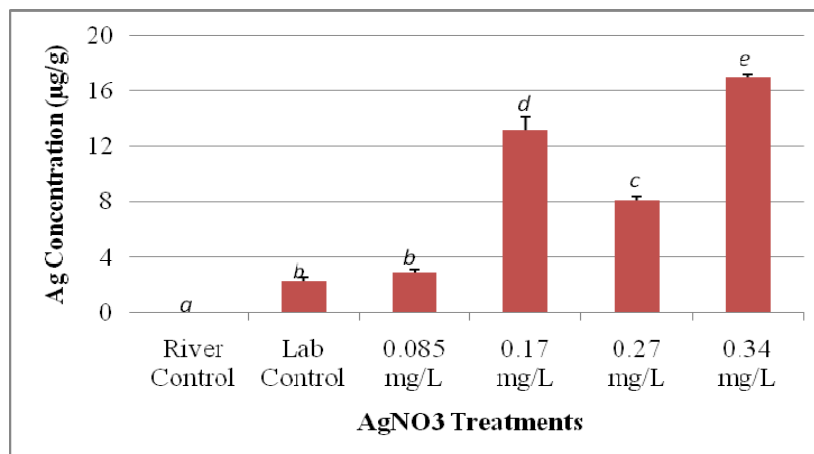


Figure 7b. Total amount of Ag (µg/g dry w.) accumulated in crayfish muscle tissue in AgNO₃ treatments as determined by GFAAS measurements. The bar graphs represent Ag content means ±SD of three measurements. Columns with different letters (*a, b, c, d, e*) are significantly different at probability level $\alpha \leq 0.05$ as determined by multiple comparison test Student-Newman-Keuls (SPSS 16.0). Each value is the mean of three measurements.

Figure 7c shows significantly different Ag content levels in all AgNP treatments when compared to river control ($\alpha \leq 0.05$). No significant difference was found between the lab control and the 0.115 mg/L concentration treatment. Additionally, each AgNP treatment demonstrated statistically significant accumulation results when compared to the other three AgNP treatments.

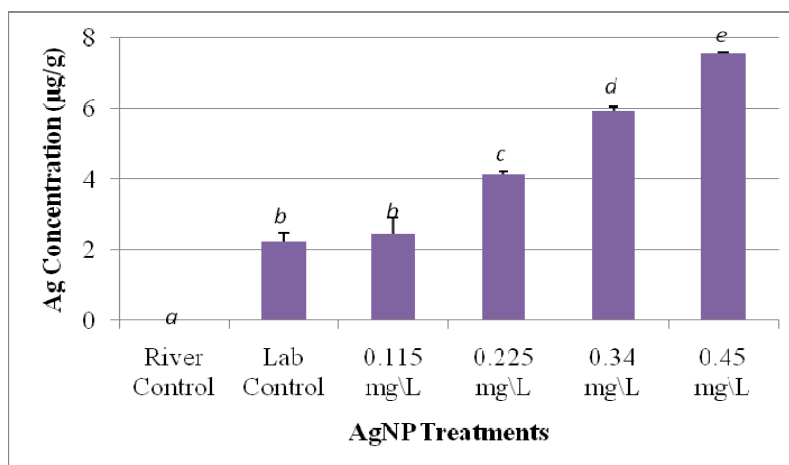


Figure 7c. Total amount of Ag ($\mu\text{g/g}$ dry w.) accumulated in crayfish muscle tissue in AgNP treatments as determined by GFAAS measurements. The bar graphs represent Ag content means \pm SD of three measurements. Columns with different letters (*a, b, c, d, e*) are significantly different at probability level $\alpha \leq 0.05$ as determined by multiple comparison test Student-Newman-Keuls (SPSS 16.0). Each value is the mean of three measurements.

DISCUSSION

The results of the comet assay (Figures 5a, 5b, and 5c) show DNA damage in brain nuclei of all treatments. In recent years comet assay has become a standard and reliable method for assessing DNA damage in the biological systems of animals, plants, and humans. The principle of this method, based on single cell gel electrophoresis, allows for detection of single and double DNA strand breakage (Frenzilli et al. 2006). DNA damage detected in our study on crayfish brain tissue exposed to AgNPs suggests that a similar response could be expected in other living organisms. The observed dose response to all experimental treatments seems to follow a nonconventional dose response. Hodgson (2004) suggests that low doses of chemical exposure stimulate a physiological response that can offset adverse effects. This compensatory response is observed as an effect opposite to toxic response at a higher levels of chemical exposure. At threshold dose, organisms respond with increased stimulation and overcompensation of toxic effect

demonstrated as a return to the zero response level or decrease in toxic effect. Continuing increased exposure levels overcome the organism's defence ability at the "pseudo" threshold level. In this study, the crayfish body's natural defenses seemed to block toxin uptake as exposure increased and less damage was observed, shown as hormesis in Figure 8. After a certain point, increased treatment exposure concentrations demonstrate the typical dose response to the toxicant, shown graphically as the near linear trend upwards. It is the pseudothreshold that is often mistaken as the actual threshold.

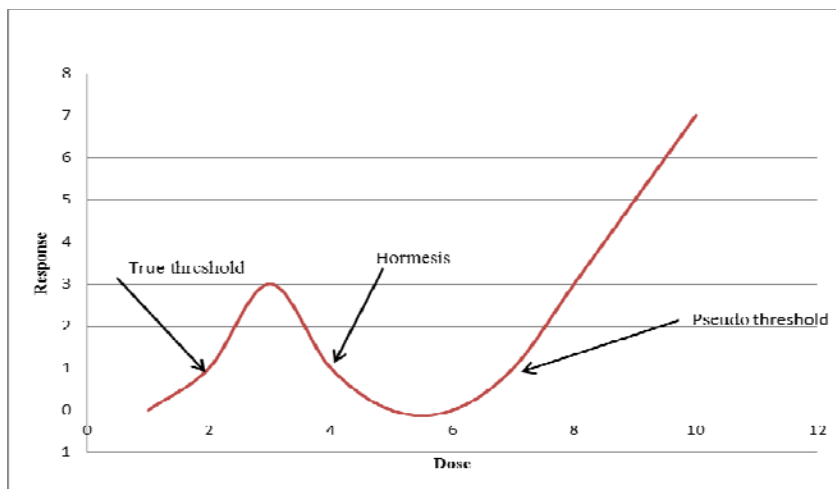


Figure 8. Hypothetical dose response to illustrate a nonconventional dose response.

The treatments resulted in the most damage to brain DNA. Figure 4 is lacking the two highest concentrations responses because the photographs taken of the slides showed either nuclei or DNA comets, but not both. The damage was so great that it was not possible to measure damage at those concentrations. Hyeon-Jin et al. (2009) considers NaBH_4 as an effective reducing agent. In the synthesis of AgNPs for this experiment, NaBH_4 was used as reducing agent to react with AgNO_3 . Unfortunately there is no literature on the ecological toxicity of NaBH_4 . There is, however, a large body of

information on toxicity of the other synthesis component, AgNO₃, on aquatic (Bianchini and Wood 2003) and terrestrial (Pelkonen et al. 2003) organisms.

Data collected in this study demonstrated that the synthesis components of AgNPs are very toxic given the mortality of crayfish in the AgNO₃ treatments (Figure 1), and cause extensive DNA damage (Figures 3 and 4). Jayabalan et al. (2008) has documented that AgNPs in colloidal solution can deaggregate to form the parental compounds. Toxicity of AgNPs in this experiment may also be attributed to the partial deaggregation of AgNPs in the experimental treatments.

Accumulation of Ag in the experimental organisms did not show any specific trend in the AgNO₃ treatments and was observed at minimal levels in the NaBH₄ treatments. The accumulation of Ag among the AgNP concentrations, however, shows an increase in Ag with increasing treatment concentration, suggesting that as nanoparticle concentration increases the uptake into the organs also increases. Bothun (2008) found that nanoparticles could freely pass through barriers in the body. The DNA damage found in the crayfish neural tissue of our experimental samples supports those findings.

CONCLUSION AND RECOMMENDATIONS

There is a clear trend of Ag accumulation found in the AgNP treatments. The near linear fit suggests that increased exposure leads to increased absorption. It is also clear that the organisms exposed to these nanoparticles showed no outward behavioral changes but were undergoing widespread DNA damage. This can be of concern to humans because extensive DNA damage can be occurring while no apparent effect is being observed.

It is of vital importance both to aquatic organisms and to humans that these materials be studied further. This experiment mirrors others in its findings that AgNPs cause DNA damage. Production of consumer goods containing this product should be placed on hold so more research can be done and the Environmental Protection Agency and the Department of Health and Human Services can issue regulations halting future exposure.

ACKNOWLEDGEMENTS

I would like express my appreciation to the Hudson River Foundation and the Tibor T. Polgar Fellowship Committee for the opportunity to conduct this research and for their support. Completion of this research would not have been possible without the supervision and mentorship of Dr. Zofia Gagnon, and I extend my sincere thanks for all her knowledge, expertise, time, and efforts. I would also like to acknowledge Dr. Neil Fitzgerald for his expertise and support and for providing access to the River Lab and to Marist College School of Science instrumentation. I also express thanks to my peers Anne Quach, Rachel Serafin, and Seth Brittle for their assistance during the research process.

LITERATURE CITED

- Ahamed, M., M. Karns, M. Goodson, J. Rowe, S.M. Hussain, J.J. Schlager, and Y. Hong. 2008. DNA damage response to different surface chemistry of silver nanoparticles in mammalian cells. *Toxicology and Applied Pharmacology* 233: 404-410.
- Bansal, R.C. and M. Goyal. 2005. *Activated Charcoal Adsorption*. Taylor and Francis, Boca Raton, FL.
- Bianchini, A. and C.M. Wood. 2003. Mechanism of acute silver toxicity in *Daphnia magna*. *Environmental Toxicology and Chemistry* 22: 1361-1367.
- Bothun, G.D. 2008. Hydrophobic silver nanoparticles trapped in lipid bilayers: size distribution, bilayer phase behavior, and optical properties. *Journal of Nanobiotechnology* 6:13, 10 pp.
- Braydich-Stolle, L., S.M. Hussain, J.J. Schlager, and M.C. Hoffman. 2005. *In vitro* cytotoxicity of nanoparticles in mammalian germline stem cells. *Toxicological Sciences* 88: 412-419.
- Chau, C.F., S.H. Wu, and G.C. Yen. 2007. The development of regulations for food nanotechnology. *Trends in Food Science Technology* 18: 269-280.
- Choi, O. and Z. Hu. 2008. Size dependent and reactive oxygen species related nanosilver toxicity to nitrifying bacteria. *Environmental Science & Technology* 42: 4583-4588.
- Creighton, J.A. and D.G. Eadon. 1991. Ultraviolet-visible absorption spectra of the colloidal spectra elements. *Journal of the Chemical Society, Faraday Transaction* 87: 3881-3892.
- Elechiguerra, J.L., J. Burt, J.R. Morones, A. Camacho-Bragado, X. Gao, H.H. Lara, and M.J. Yacaman. 2005. Interaction of silver nanoparticles with HIV-1. *Journal of Nanobiotechnology* 3: 6. doi:10.1186/1477-3155-3-6
- Frenzilli, G., V. Scarcell, F. Fornal, A. Paparelli, and M. Nigro. 2006. The comet assay as a method of assessment of neurotoxicity. *Annals of the New York Academy of Science* 1074: 478-480.
- Gosheger, G., J. Hades, H. Ahrens, A. Streitburger, H. Buerger, M. Erren, A. Günsel, F.H. Kemper, W. Winkleman, and C. von Eiff. (2004). Silver-coated megaendoprostheses in a rabbit model—an analysis of the infection rate and toxicological side effects. *Biomaterials* 25: 5547–5556.
- Hagfeldt, A. and M. Graetzel. 1995. Light-induced redox reactions in nanocrystalline systems. *Chemical Reviews* 95(1): 49–68. doi: 10.1021/cr00033a003.

- Henig, R.M. Our silver-coated future. *OnEarth* September 1, 2007: 22–29.
- Hodgson, E. 2004. *A Textbook of Modern Toxicology*. Wiley-Interscience, Hoboken, NJ.
- Hornyak, G.L., H.F. Tibbals, J. Dutta, and J.J. Moore. 2009. *Introduction to Nanoscience and Nanotechnology*. CRC Press, Boca Raton, FL.
- Hussain, S.M., K.L. Hess, J.M. Gearhart, K.T. Geiss, and J.J. Schlager. 2005. *In vitro* toxicity of nanoparticles in BRL, 3A rat liver cells. *Toxicology in Vitro* 19: 975-983.
- Hyeon-Jin, S., K.K. Kim, A. Benayad, S. Yoon, K.P. Hyeon, I. Jung, M.H. Jin, H.K. Jeong, J. Kim, J. Choi, and Y.H. Lee. 2009. Efficient reduction of graphite oxide by sodium borohydride and its effect on electrical conductance. *Advanced Functional Materials* 19: 1987–1992.
- Jayabalan, J., A. Singh, R. Chari, H. Srivastava, P.K. Mukhopadhyay, A.K. Srivastava, and S.M. Oak. 2008. Aggregated nanoplatelets: optical properties and optically induced disaggregation. *Journal of Physics: Condensed Matter* 20(44). doi: 10.1088/0953-8984/20/44/445222.
- Kim, J.S., E. Kuk, K.N. Yu, J.H. Kim, S.J. Park, H.J. Lee, S.H. Kim, Y.K. Park, Y.H. Park, C.Y. Hwang, Y.K. Kim, Y.S. Lee, D.H. Jeong, and M.H. Cho. 2007. Antimicrobial effects of silver nanoparticles. *Nanomedicine* 3: 95–101.
- Larese, F.F., F. D’Agostin, M. Crosera, G. Adami, N. Renzi, M. Bovenzi, and G. Maina. 2009. Human skin penetration of silver nanoparticles through intact and damaged skin. *Toxicology* 255: 33-37.
- Mnyusiwalla, A., A.S. Daar, and P.A. Singer. 2003. ‘Mind the gap’: science and ethics in nanotechnology. *Nanotechnology* 14(3): 14 R9-R13 doi:10.1088/0957-4484/14/3/201.
- Moghimi, S.M., A.C. Hunter, and J.C. Murray. 2001. Long-circulating and target-specific nanoparticles: theory to practice. *Pharmacological Reviews* 53: 283–318.
- Paddle-Ledinek, J.E., Z. Nasa, and H.J. Cleland. 2006. Effect of different wound dressings on cell viability and proliferation. *Plastic and Reconstructive Surgery* 117: 110S–118S.
- Panyam, J. and V. Labhasetwar. 2003. Biodegradable nanoparticles for drug and gene delivery to cells and tissue. *Advanced Drug Delivery Reviews* 55: 329–347.

- Pelkonen, K.H., H. Heinonen-Tanski, and O.O. Hanninen. 2003. Accumulation of silver from drinking water into cerebellum and musculus soleus in mice. *Toxicology* 186: 151-157.
- Ringer, S.P and K.R. Ratinac. 2004. On the role of characterization in the design of interfaces in nanoscale materials technology. *Microscopy and Microanalysis* 10: 324–335.
- Samuel, U. and J.P. Guggenbichler. 2004. Prevention of catheter-related infections: the potential of a new nano-silver impregnated catheter. *International Journal of Antimicrobial Agents* 23: 75–78.
- Sung, J.H., J.H. Ji, J.U. Yoon, D.S. Kim, M.Y. Song, J. Jeong, B.S. Han, J.H. Han, Y.H. Chung, J. Kim, T.S. Kim, H.K. Chang, E.J. Lee, J.H. Lee, and I.J. Yu. 2008. Lung function changes in Sprague-Dawley rats after prolonged inhalation exposure to silver nanoparticles. *Inhalation Toxicology* 20: 567-574.
- The Center for Food Safety. “Nanotechnology: It’s a small (and unregulated) world after all.” *Food Safety Now!* Autumn 2006.
- Ulkur, E., O. Oncul, H. Karagoz, E. Yeniz, and B. Celikoz. 2005. Comparison of silver-coated dressing (Acticoat), chlorhexidine acetate 0.5% (Bactigrass), and fusidic acid 2% (Fucidin) for topical antibacterial effect in methicillin-resistant *Staphylococci*-contaminated, full-skin thickness rat burn wounds. *Burns* 31: 874–877.
- Usui, H., H. Matsui, N. Tanabe, and S. Yanagida. 2004. Improved dye-sensitized solar cells using ionic nanocomposite gel electrolytes. *Journal of Photochemistry and Photobiology A: Chemistry* 164: 97-101.
- Vigneshwaran, N., A.A. Kathe, P.V. Varadarajan, R.P. Nanchane, R.H. Balasubramanya. 2007. Functional finishing of cotton fabrics using silver nanoparticles. *Journal of Nanoscience and Nanotechnology* 7: 1893-1897.
- Woodrow Wilson International Center for Scholars. 2007. A nanotechnology consumer products inventory. Online at <http://www.nanotechproject.org/consumerproducts>.
- Ying, J. 2001. *Nanostructured Materials*. Academic Press, New York.